Optical study of $Al_{0.4}Ga_{0.6}Sb/GaSb$ single quantum wells

R. Ferrini, M. Geddo, G. Guizzetti, and M. Patrini
INFM-Dipartimento di Fisica, ''A. Volta,'' Università di Pavia, Via Bassi 6, I-27100 Pavia, Italy

S. Franchi and C. Bocchi
CNR-MASPEC Institute, Via Chiavari 18, I-43100 Parma, Italy

E. Kh. Mukhamedzhanov
A.V. Shubnikov's Institute of Crystallography of Russian Academy of Sciences, Leninskiy Prospekt 59, RUS-11733 Moscow, Russia

A. Baraldi and R. Magnanini
INFM-Dipartimento di Fisica, Università di Parma, Viale delle Scienze, I-43100 Parma, Italy
(Received 18 November 1998)

Despite the recent upsurge in research on GaSb-based systems, only few systematic investigations have been performed on the fundamental optical and electronic properties of $Al_xGa_{1-x}Sb/GaSb$ quantum wells. For this reason we studied a series of $Al_{0.4}Ga_{0.6}Sb/GaSb$ single quantum wells, with well thicknesses ranging from 40 to 117 Å, by reflectance (R) and photoreflectance (PR) in the 0.6 to 1.5 eV spectral range and at temperatures from 6 to 300 K. The structures were grown by molecular-beam epitaxy on (001) GaSb substrates and structurally and compositionally characterized by photoluminescence, x-ray diffraction, and reflection high-energy electron diffraction. Both R and PR spectra showed clear evidence of the structures associated with the transitions allowed between the nth heavy-(light-) hole subband and the nth conduction subband for $n=1$ and 2. Standard critical-point line shapes fitted satisfactorily the PR structures, allowing accurate determination of both transition energies and broadening parameters as functions of the well thickness. The transition energies were well fitted by a theoretical model based on the envelope-function scheme, thus giving reliable values for the two fit parameters, i.e., the band offset and the conduction-band nonparabolicity. [S0163-1829(99)05423-5]

I. INTRODUCTION

The optical and electronic properties of quantum wells and superlattices involving GaSb-based alloys have recently attracted increasing interest for their potential application in devices, especially in high-power $Al_xGaAs_{1-x}Sb/GaSb$ laser emitters at 3–4 μm,[1] normal-incidence infrared (5–15 μm) photodetectors[2] and modulators[3] based on interconduction subband transitions in $GaSb/Al_xGa_{1-x}Sb$ multiquantum wells (MQW's). Thus a great effort has been made to satisfy the need for novel experimental and theoretical results. Nevertheless, only few papers[4–6] have analyzed in detail the optical intersubband transitions in $Al_xGa_{1-x}Sb/GaSb$ quantum wells (QW's) and correlated them with the electronic structure of QW's as a function of one or more parameters, such as well thickness (t_W), strain, band offset, effective masses, and conduction-band nonparabolicity. Moreover, there is still a certain diversity in the band-parameter values from these papers and, more generally, from literature.[7]

In the experimental works, absorption spectroscopy,[4] electroreflectance[5] (ER), and photoluminescence[4,6] (PL) have generally been used, while photoreflectance (PR) and reflectance (R) have rarely appeared, even if they have been extensively and successfully applied to characterizing and studying the fundamental properties of other III-V semiconductor quantum-size structures.[8] A reason for the scarce use of PR is that difficulties are often encountered when exploiting the modulation efficiency in bulk and epitaxial Sb-based semiconductors, so that only two papers,[9,10] which came to partially divergent conclusions, have dealt with this topic. In a recent work[11] we gave experimental evidence of a strong PR effect in $GaSb/Al_xGa_{1-x}Sb$ single quantum wells (SQW's), and we showed that even unintentionally doped GaSb-based quantum systems can be studied and characterized by PR. Optical-absorption spectroscopy has in turn been systematically preferred to R as a probe of layered GaSb compounds, although it requires transparent substrates (e.g., GaAs), which may induce significative strain effects due to the strong lattice mismatch ($\sim 7\%$) between GaAs and GaSb.

Here we present a systematic PR and R study from 0.6 to 1.5 eV and at different temperatures on a series of unintentionally doped $Al_{0.4}Ga_{0.6}Sb/GaSb$ SQW's with different well thicknesses. In order to reduce the strain effects, the samples were grown by molecular-beam epitaxy (MBE) on (001) GaSb substrates and were well characterized in composition, crystalline structure, thicknesses, and interfaces by photoluminescence, reflection high-energy electron diffraction (RHEED), and high-resolution x-ray diffraction (HRXRD). We chose the mole fraction $x=0.4$ for the $Al_xGa_{1-x}Sb$ layers since this is the composition generally used for quantum well infrared photodetectors.

The aims of this work are to clearly evidence the optical transitions between quantum states in the SQW's and to precisely determine their energies for subband index $n \geqslant 1$, to compare the experimental energies with theoretical values obtained with a model based on the envelope-function scheme, and to give more reliable information on character-

0163-1829/99/59(23)/15395(7)/$15.00 PRB 59 ©1999 The American Physical Society

istic parameters such as band offset and GaSb conduction-band nonparabolicity, whose values heavily influence the electronic structure of these systems.

II. EXPERIMENTS

The structures were grown by MBE in an Intevac Gen II modular growth chamber on (001) GaSb substrates using a Sb_4 molecular beam. They consisted of 500-nm-thick GaSb buffers and of $Al_{0.4}Ga_{0.6}Sb$/GaSb SQW's. In order to maximize the PL quantum efficiency of the QW's, the buffers were grown at 450 °C, except in the topmost part, where the temperature was linearly increased up to 550 °C and then stabilized for the growth of QW's. The $Al_{0.4}Ga_{0.6}Sb$ and GaSb growth rates were 1.0 and 0.6 μm/h, respectively, and the Sb_4/Ga beam equivalent pressures (BEP's) were in the 10–14 range.

The growth rates were deduced by analyzing the RHEED oscillations that were carried out prior to the growth of each QW structure and have an accuracy to within $\pm 5\%$. Using the values of GaSb and $Al_xGa_{1-x}Sb$ growth rates, the growth times were established so as to have the following values. For the thicknesses of the two barriers, 200 and 500 Å towards the surface and the substrate, respectively, and for the wells, $t_W = 40$, 60, 80, and 117 Å in samples 40, 60, 80, and 117, respectively. Adjusting the growth rates predetermined the composition.

The structures were characterized by means of PL excited at 10 K by the blue line of an Ar^+ laser with a power density of 5 W/cm^2 and using a Fourier-transform spectrometer and a cooled Ge detector.

HRXRD experiments were carried out in conventional $(n,-n)$ double crystal geometry by means of a computer controlled diffractometer using $CuKa_1$ radiation and 004 reflection. A Rigaku RU-200 rotating anode generator was used as the radiation source. The incident beam was conditioned by a *U*-shaped (004) Si monochromator. In order to reduce the diffuse scattering background of the sample, a thin slit on the detector with an acceptance angle of nearly 0.4° was used, and the measurements were carried out in the w-$2q$ scan mode. The rocking curves were recorded in a wide angular range, from -3000 to 3000 arcsec, because the effect of the abruptness of the interfaces on the diffraction profile was clearly visible far from the Bragg peaks. The intensity modulations and angular positions of the interference fringes (Pendellösung) in the x-ray diffraction profiles were fitted by means of a suitable calculation program based on the dynamic theory of x-ray diffraction. With this procedure it is generally possible to determine the structural parameters (strain, thickness, abruptness of interfaces, and chemical composition) of the whole heterostructure, even if the constituent layers are on a nanometer scale. Details on the growth conditions as well as on the optical and morphological characterization of GaSb and $Al_xGa_{1-x}Sb$ epitaxial layers have been reported elsewhere.[12–14]

PR measurements were performed at near-normal incidence in the 0.7–1.5 eV photon energy range, with energy step and spectral resolution of 1 meV. The standard experimental apparatus[15] operated with a 100 W halogen lamp as probe source. The excitation source was provided by a 2 mW He-Ne laser ($\lambda = 632.8$ nm) mechanically chopped at a frequency of 220 Hz. The pump beam was guided to the sample by an optical fiber allowing greater flexibility in the optical layout. The samples were mounted in thermal contact with the cold finger of a microminiature Joule-Thompson refrigerator coupled with a programmable temperature controller, allowing measurements in the 80–300 K temperature range. The reproducibility of the PR signal versus position on the sample was checked by scanning the surface through microstep movements of an x-y stage.

R at near-normal incidence was measured in the 0.6–1.5 eV photon energy range by a Cary 5E automatic spectrophotometer, with a photometric accuracy of 0.5% and spectral resolution better than 0.2%. An Al mirror covered with a MgF_2 film, whose absolute reflectivity was directly measured, was used as reference. The samples were put on the cold finger of a helium flow cryostat and measured at several different temperatures between 6 and 300 K.

TABLE I. Upper (towards the surface) and lower (towards the substrate) Al content in $Al_xGa_{1-x}Sb$ barriers, and effective well thicknesses (in Å) measured by HRXRD.

Sample No.	x (upper barrier)	x (lower barrier)	Elective well thickness t_x (Å)
40	0.427 ± 0.005	0.424 ± 0.005	31.5 ± 1.0
60	0.418 ± 0.005	0.417 ± 0.005	49.8 ± 1.0
80	0.397 ± 0.005	0.391 ± 0.005	74.5 ± 1.5
117	0.406 ± 0.005	0.403 ± 0.005	105.6 ± 2.0

III. RESULTS AND DATA ANALYSIS

Table I shows the parameters of the wells and the barriers obtained by fitting the HRXRD experimental curves under the assumption that the QW structure is made up of three layers consisting of the two barriers and the well. Slightly better fits are obtained when the structure is considered as constituted by five or six layers, thus suggesting that the interfaces are not abrupt. This may explain the discrepancy between the intended values and the HRXRD values of the effective well thicknesses given in Table I. The composition of the barrier layers were obtained by taking into account the deviation from the Vegard law found in a recent study[16] of the $Al_xGa_{1-x}Sb$ on GaSb epitaxial system. The value of the composition x has been calculated using the equation

$$x = 0.0947\xi^2 + 0.9048\xi - 0.000213, \tag{1}$$

where ξ is the value of the composition evaluated from the x-ray diffraction measurement of the lattice parameter by using the Vegard law.

The energies of the PL peaks (Fig. 1) were fully consistent with those of a large number of pseudomorphic QW's with the same barrier composition and grown under the same conditions. The full widths at half maxima (FWHM's) of PL peaks were at least as wide as those reported in the literature and relatively large (e.g., 8 meV for sample 80), thus suggesting that the interfaces were relatively rough compared to those of the $Al_xGa_{1-x}As$/GaAs system. This is qualitatively consistent with the HRXRD results described above.

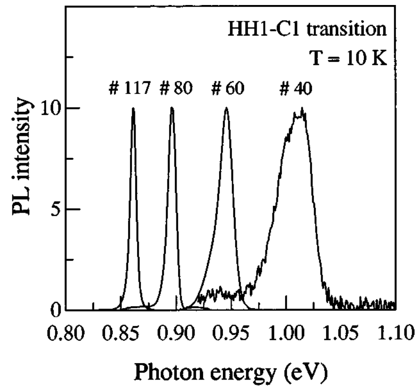

FIG. 1. 10 K photoluminescence spectra of $Al_{0.4}Ga_{0.6}Sb$/GaSb SQW's samples with different well thicknesses. Peaks correspond with the intersubband HH1-C1 transition.

Growth interruptions at the heterointerfaces, which in other systems are beneficial for the reduction of the interface roughness, do not seem to have much effect. The $Al_xGa_{1-x}Sb$/GaSb interface roughness causes the relatively large value (e.g., 12 meV at 10 K for sample 60) of the Stokes shift between the exciton peaks, which were measured by reflectance techniques and PL. This can be interpreted as due to exciton localization in the widest parts of the QW's.

In Fig. 2 we present the PR spectra (solid lines) of samples 40, 60, 80, and 117, taken at 90 K in the 0.75–1.45 eV range, and the corresponding best fits (dashed lines) obtained according to the line-shape models characteristic of PR spectroscopy[17,18] (see below). For clarity, 60, 80, and 117 spectra were shifted vertically with respect to 40 spectrum.

Low- and high-energy arrows mark the features due to the direct energy gap (E_0) of the GaSb buffer layer and of the $Al_{0.4}Ga_{0.6}Sb$ barrier, respectively, and which correspond to

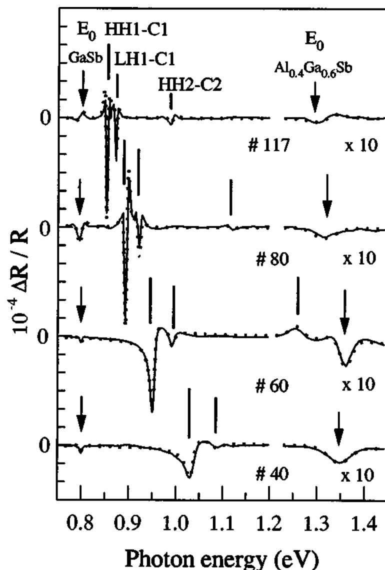

FIG. 2. 90 K photoreflectance spectra of all samples (solid lines) and best fits of the optical spectra (dashed lines) to standard *CP* line shape. Arrows (E_0 of GaSb and $Al_{0.4}Ga_{0.6}Sb$ layers) and bars (HH1-C1, LH1-C1, and HH2-C2) mark the fitted transition energies. For clarity, the spectra were shifted vertically with respect to sample 40 spectrum.

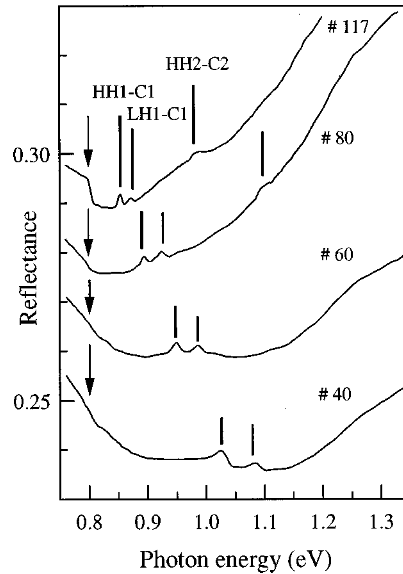

FIG. 3. 90 K reflectance spectra of all samples. Arrows mark the energy positions of the E_0 gap of GaSb buffer layer. Bars indicate the R features due to the HH1-C1, LH1-C1, and HH2-C2 transitions in GaSb wells. For clarity, both samples 60 and 117 spectra were shifted vertically by 0.02 with respect to samples 40 and 80 spectra, respectively.

the M_0 tridimensional critical point (Γ_8-Γ_6 transition) in the joint density of states.[8,9,14] The temperature behavior of these spectral features (see Ref. 11) was in excellent agreement with thermoreflectance results[19] from high-quality GaSb and $Al_xGa_{1-x}Sb$ single layers grown by MBE in the same chamber.

In addition to the PR features due to the bulk band gaps, other spectral features are clearly displayed in Fig. 2. If HHn-(LHn-) Cn indicates the transitions from the nth heavy-(light-) hole quantum level to the nth confined level of the conduction band in the quantum well region of the samples, these features can be attributed to the HH1-C1, LH1-C1, and HH2-C2 direct transitions at Γ point on the basis of the following characteristics: their energy location, the energy dependence on the well width and on the temperature (with decreasing temperature they blueshift by the same amount as the gap of the well material,[11] while LH1-HH1 splitting remains almost constant), as well as the agreement with the energy-level calculation discussed below.

Figure 3 shows the normal-incidence R spectra of the same samples, taken at 90 K in the 0.75–1.35 eV range, which display features corresponding to those of PR. For clarity, both samples 60 and 117 spectra were shifted vertically by 0.02 with respect to samples 40 and 80 spectra, respectively. The R low-energy shoulder (arrows), which is partially influenced by the interference effects of the layered structure, marks the E_0 gap of the GaSb buffer layer. In the case of sample 117, where it is particularly evident, the E_0 value is in excellent agreement with the thermoreflectance results of Refs. 14 and 19. The R high-energy shoulder is related to the E_0 energy gap of the $Al_{0.4}Ga_{0.6}Sb$ barriers. A couple of peaks appear between the fundamental absorption edges of barrier and well in all spectra. Their energy position and separation, as well as the broadening, increase with decreasing t_W. A third peak is clearly visible in the spectra of

TABLE II. (Al,Ga)Sb material parameters used in the envelope-function calculation of the QW transition energies.

Parameter (unit)	Sample No.	Value	Remarks
GaSb E_0 gap (eV)		0.799	PR measurements
$Al_xGa_{1-x}Sb$ E_0 gap (eV)	40	1.348	
	60	1.357	PR measurements
	80	1.312	
	117	1.320	
Spin-orbit splitting Δ_0 (eV)		$0.76-0.39\,x+0.3\,x^2$	Ref. 32
Valence-band offset ΔE_v (meV)		160	Ref. 33
GaSb effective masses (m_0)		$m_c=0.04$	
		$m_{hh}=0.27$	Refs. 5 and 6
		$m_{lh}=0.045$	
$Al_xGa_{1-x}Sb$ effective masses (m_0)		$m_c\{1+7.74[2/E_0+1/(E_0+\Delta_0)]\}^{-1}$	
		$m_{hh}=0.27+0.18\,x$	Refs. 5 and 6
		$m_{lh}=0.045+0.085\,x$	
GaSb CB nonparabolicity parameter E_{0C} (eV)		0.989 (T=0 K)	
		0.974 (T=90 K)	Ref. 26

samples 80 and 117. These three peaks correspond to the HH1-C1, LH1-C1, and HH2-C2 direct transitions: in particular, the HH2-C2 structure does not appear in the R spectrum (or in the PR spectrum) of sample 40 because the C2 level falls in the continuum, while in sample 60 the HH2-C2 structure is smeared in the high-energy shoulder because of the nearness of the absorption edge of $Al_{0.4}Ga_{0.6}Sb$.

Since the optical spectra display features due both to bulk interband transitions and to quantum-size intersubband transitions, in order to precisely determine the corresponding energies we first fitted the PR data to the line-shape models most appropriate to the nature of the transitions.

As far as the interband transitions are concerned, in bulk semiconductors in the low-field limit, near a critical point (CP) the modulated reflectance signal ($\Delta R/R$) is characterized by a third-derivative-like behavior of the complex dielectric function ($\tilde{\epsilon}$) with respect to the photon energy $\hbar\omega$.[20,21] Since the low-field limit is satisfied in PR if Franz-Keldysh oscillations are absent (i.e., for native surface electric field $\leqslant 10^4$ V/cm), the CP energy E_C can be obtained by fitting the PR line shape by the Aspnes functional form[20]

$$\Delta R/R=\mathrm{Re}[Ae^{i\phi}(\hbar\omega-E_C+i\gamma)^{-m}], \quad (2)$$

where A and ϕ are, respectively, the amplitude factor and the phase projection angle that vary slowly with $\hbar\omega$; γ is the Lorentzian broadening parameter for the CP; m is an integer or half-integer depending on the CP type ($m=2.5$ for a three-dimensional interband CP, $m=3$ for a two-dimensional CP). In Table II we report the E_0 energies derived from the best fit to the PR structures both in GaSb buffers and in $Al_{0.4}Ga_{0.6}Sb$ barriers.

For the intersubband transitions, it is worth noting that in quantum-size structures PR is a first-derivative spectroscopy.[8] It was shown[17] that for a bidimensional CP (allowed intersubband transitions) in the absence of excitonic effects the first derivative of $\tilde{\epsilon}$ with respect to $\hbar\omega$ produces the same $\Delta R/R$ line shape as Eq. (2) with $m=1$. It was found that, when excitonic effects cannot be neglected, as in the GaAs-based QW's even at room temperature,[22–24] a Gaussian broadening (involving hypergeometric functions)[8] is more appropriate than a Lorentzian broadening[20] [Eq. (2) with $m=2$] in the related $\tilde{\epsilon}$. However, Shanabrook and co-workers[22] showed that the third-derivative functional form for a two-dimensional CP [i.e., Eq. (2) with $m=3$] does mimic the first derivative of the Gaussian dielectric function and can be used as a reasonable and useful approximation, due to its closed analytical form.

We therefore performed the least-square fit of PR spectra by using the Eq. (2) with $m=2.5$, 1, or 3 to reproduce in order, a bulk interband transition, a QW intersubband (Lorentzian) transition and a QW excitonic (Gaussian) transition. The best fits well reproduce the experimental line shapes in all samples, thus supporting our attributions of the spectral features. The energies and the broadenings derived from the best fit to the HH1-C1, LH1-C1, and HH2-C2 structures are listed in Table III, together with the energies deduced from R measurements, corresponding with the peak energy positions at $T=90$ K.

IV. DISCUSSION

While the fitted values of the E_0 gap in the different GaSb buffer layers coincide within the experimental accuracy (± 1 meV), we obtained four different values for E_0 in the $Al_{0.4}Ga_{0.6}Sb$ barrier layers (see Table II), corresponding with different effective compositions x. On the other hand, these E_0 values differ by less than 1% with respect to those obtained from thermoreflectance measurements on $Al_xGa_{1-x}Sb$ thick and relaxed layers (see Ref. 19): apart from experimental uncertainty, this small difference is due to the fact that in our case the $Al_{0.4}Ga_{0.6}Sb$ barrier layers were pseudomorphically grown on the GaSb layers, as it is suggested by Ref. 25, and they were slightly strained (the typical lattice mismatch between GaSb and $Al_{0.4}Ga_{0.6}Sb$ is only $\Delta a/a\sim 0.27\%$).[6] It was also of interest that the PR line shapes corresponding to the E_0 gap of both GaSb buffer layers and $Al_xGa_{1-x}Sb$ barriers of samples 40 and 60 differ slightly from those of samples 80 and 117: this is due to the different values of

TABLE III. Energy and broadening parameter values (in meV) derived from the best fit of the 90 K PR structures due to the HH1-C1, LH1-C1, and HH2-C2 QW transitions. The energies of the equivalent R peaks are also reported.

Sample	Photoreflectance						Reflectace		
No.	HH1-C1	γ	LH1-C1	γ	HH2-C2	γ	HH1-C1	LH1-C1	HH2-C2
40	1034	9.5	1087	10.0			1028	1082	
60	952	5.5	992	6.0	1260	18.0	948	988	
80	894	3.9	921	4.5	1115	7.5	894	924	1112
117	852	3.0	872	3.3	989	7.2	854	872	989

phase ϕ in Eq. (2), which are due to different optical paths in the multilayer structures.[17]

The 90 K PR features due to the QW transitions (HH1-C1, LH1-C1, and HH2-C2) are characterized by a band-to-band line shape in samples 40 and 60 [$m=1$ in Eq. (2)] and by an excitonic line shape in samples 80 and 117 [$m=3$ in Eq. (2)]. In spite of this, the analysis of the spectral features at different temperatures indicates that even for samples 80 and 117 the excitonic character of the transitions is lost for $T\geqslant 250$ K. This can be explained both by thermal effects and interface roughness.

We remind that the exciton binding energy in bulk GaSb is much smaller than in bulk GaAs (1.5 vs 3.8 meV) and that the same ratio applies in the bidimensional limit: thus the confined excitons in GaSb wells are more drastically affected by thermal effects with respect to similar GaAs-based heterostructures,[11,26] where it was shown that the QW interband transitions are excitonic even at room temperature.[23,27] Nevertheless, the different behavior of samples 80 and 117 indicates that in GaSb-based QW's temperature alone cannot be responsible for ionizing confined excitons. We believe that this different behavior is due to the nonabruptness of $Al_xGa_{1-x}Sb$/GaSb interfaces, which involved 3–5 monolayers of the GaSb wells, according to HRXRD analysis. The low quality of the first few monolayers should induce a great density of defects and complexes, which, in turn, are known to produce high density of p-type impurities ($\geqslant 10^{17}$ cm^{-3} in GaSb bulk samples).[13,28] The enhanced free-carrier concentration causes partial exciton screening and, combined with thermal disorder, makes band-to-band transitions more favorable than excitonic ones. This happens particularly in the thinnest wells (i.e., samples 40 and 60), while in samples 80 and 117 the nonintentional free carriers are indeed distributed in a wider well and their effective density is lowered.

An interesting point is the different broadening γ of the QW spectral structures observed in the four samples. The HH1-C1, LH1-C1, and HH2-C2 structures become stronger and sharper as well thickness is increased. It is well known that interface roughness broadens the linewidth of thinner wells more substantially: for the ideal case of an infinite-barrier-height square well, a $1/t_W{}^3$ dependence of the linewidth on the well width t_W is expected.[29] However, theoretical studies[30] have shown that both interface roughness and alloy disorder cause a more complicated dependence of the linewidth on microstructural parameters and the decay is smoother (i.e., the exponent of t_W is considerably smaller). Our results are consistent with this observation (the broadening varies with $\sim 1/t_W{}^{1.2}$) and confirm the PL evidence of the lower quality of the GaSb/$Al_xGa_{1-x}Sb$ interfaces with respect to the GaSb/$Al_xGa_{1-x}Sb$ ones.

We would like to point out that the small gap ($\sim$80 meV) between the Γ and L conduction-band minima of the GaSb and the different effective masses of the electrons occupying the two valleys are expected to produce a Γ-L crossover of the conduction ground states for the thinnest wells ($\sim$36 Å for a barrier composition $x=0.31$).[6] By a more detailed study (not discussed here) of our samples PL emission as a function of t_W, it can be argued that for sample 40 the $n=1$ L quantum state is localized $\sim$30 meV below the corresponding Γ quantum state. Nevertheless R and PR data are linked to the Γ valley, i.e., they reveal essentially direct transitions; in particular the $\Delta R/R$ spectral features due to indirect transitions are weak and have no longer a derivative behavior.[31] Actually it must be noted that in the thinnest wells, besides the interface roughness effects, the proximity of the L valley may affect the broadening of the R and PR spectral features.

To compare the experimental and the theoretically predicted quantum transition energies of the $Al_{0.4}Ga_{0.6}Sb$/GaSb SQW's, we calculated the theoretical energies by means of the envelope-function model.[29] For the sake of simplicity, we used the average values of the barrier compositions reported in Table I. We believe that this procedure does not affect the results of the analysis, since the differences between the compositions of the two barriers are generally within the experimental error. The accepted values of material parameters used in the model are given in Table II.[5,6,26,32,33] We made allowance for the typical composition and thickness uncertainties, derived from HRXRD for t_W and x. We used the band-gap energies of GaSb and $Al_{0.4}Ga_{0.6}Sb$ directly obtained from the fit of PR measurements. In this way we took into account the strain effects on the band gap of the $Al_{0.4}Ga_{0.6}Sb$ barriers, which were pseudomorphically grown on the GaSb layers.[6,25] Because of the absence in the PR spectra of the strain-induced HH-LH band splitting of the $Al_{0.4}Ga_{0.6}Sb$ E_0 gap, it can be deduced that the contribution of the (001) uniaxial stress is negligible. On the other hand, we assumed that most of the hydrostatic part of the strain affects the conduction band of the barriers, thus adopting the idealized nonstrained case for the valence-band offset ΔE_v.[6] For a preliminary calculation ΔE_v was taken to be 160 meV,[33] consistent with the zero strain value of $(300\pm 75)x$ meV obtained in Ref. 6. We took the split-off band correction into consideration both in the wells and in the barriers, and we assumed for the spin-orbit splitting energy Δ_0 the values reported in Ref. 32. The calculations included the differences in effective-mass parameters between well

and barrier materials,[5,6] and the nonparabolicity of the bulk conduction band of GaSb. In Ref. 26 it was demonstrated that near Γ point the energy dispersion of the GaSb conduction band is well expressed by a Kane's model dispersion law, approximated to k^4,

$$E_C(k)=E_0+\frac{\hbar^2k^2}{2m_C}\left(1-\frac{1}{E_{0C}}\frac{\hbar^2k^2}{2m_C}\right), \quad (3)$$

where m_C is the electron effective mass and $E_{0C}=E_0/\delta$ is the conduction-band nonparabolicity parameter, while δ is the adimensional nonparabolicity coefficient. From the fitting of the optical absorption near the fundamental absorption edge, using GaSb parameters in accordance with those of Table II, Ghezzi *et al.*[26] obtained the values $\delta=0.82$. Assuming $E_0=0.799$ eV, derived from the PR measurements in our samples, we obtained the nonparabolicity parameter value $E_{0C}=0.974$ eV.

The excitonic effects that appear in samples 80 and 117 were taken into account by subtracting the exciton binding energy E_b from the calculated transition energies. The binding energy of the GaSb confined excitons was calculated by Giugno *et al.*[34] for GaSb/$Al_{0.31}Ga_{0.69}Sb$ QW's, using GaSb and $Al_xGa_{1-x}Sb$ parameters in accordance with those of Ref. 6. For the HH1-C1 confined exciton they obtained an E_b value ranging from 5.5 to 4.5 meV for t_W ranging from 30 to 120 Å. Taking into account that for the fundamental exciton state 1*s* E_b is expected to increase as x is increased ($\Delta E_b \sim 10\%$ if x is doubled in GaAs/$Al_xGa_{1-x}As$ QW's),[35] and that the difference between E_b(HH1-C1) and E_b(LH1-C1) is less than 1 meV,[35] we assumed an average value of 6 meV for the binding energies in samples 80 and 117.

Among the input parameters of the envelope-function model (i.e., the conduction- and valence-band parameters of the constituent materials and the structural parameters of the QW's), the band offset and the GaSb conduction-band nonparabolicity are the least reliable. In addition to this, preliminary calculations showed that slight variations in these two parameters strongly influence the resulting transition energies (for the other parameters we obtained differences of $\sim$1 meV). On this basis we fitted the described model to our experimentally derived transition energies, assuming ΔE_v and E_{0C} as free parameters. The least-square fit, giving a χ^2 value less than 50, was carried out using the CERN library *MINUIT* program, based on the Metropolis algorithm. The fitted curves for the HH1-C1, LH1-C1, and HH2-C2 transition energies versus t_W are shown in comparison with our PR results in Fig. 4. From the fit we obtained $\Delta E_v=156$ meV and $E_{0C}=977$ meV, in good agreement with the values of $\Delta E_v=120\pm30$ meV (Ref. 6) or $\Delta E_v=160$ meV (Ref. 33) and of $E_{0C}=974$ meV (Ref. 26).

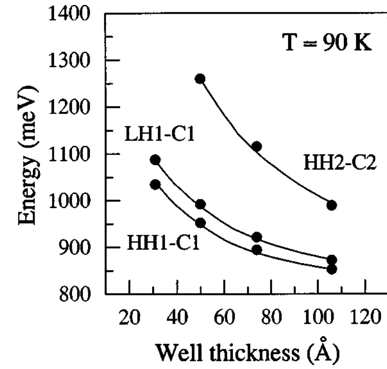

FIG. 4. 90 K transition energies in $Al_{0.4}Ga_{0.6}Sb$/GaSb SQW's as a function of the well width: experimental data (dots); theoretical calculation (solid lines).

V. CONCLUSIONS

We present an optical investigation of fully characterized $Al_{0.4}Ga_{0.6}Sb$/GaSb SQW's, conducted by using PL, R, and PR in a complementary fashion. R and PR clearly evidenced the quantum transitions HH1-C1, LH1-C1, and HH2-C2 between the valence subband and conduction subband levels. We can thus confirm the possibility of successfully applying R and PR techniques even to GaSb-based quantum confined systems, in contrast with what has been stated in previous experimental references.[10]

The line-shape broadening of the PR structures varies approximately with $1/t_W$, rather than with the ideal behavior of $1/t_W{}^3$, due to interface roughness and alloy disorder. In agreement with the PL measurements performed on the same samples, PR results confirmed that the quality of the GaSb/$Al_xGa_{1-x}Sb$ interfaces was lower than that of the GaAs/$Al_xGa_{1-x}As$ ones.

We fitted the energies calculated in the envelope-function scheme to those experimentally derived from R and PR, assuming the effective well thickness and composition obtained from the HRXRD and RHEED analysis. The parameter values we obtained for the valence-band offset and for the GaSb conduction-band nonparabolicity are thus more reliable than those so far reported in the literature.

ACKNOWLEDGMENTS

This work was partially supported by the CNR-MADESS II Project and INFM Network ''Fisica e tecnologia dei semiconduttori III-V.'' The authors would like to thank Professor L.C. Andreani for helpful discussions and generous support in theoretical calculations.

[1] P.S. Dutta, H.L. Bhat, and V. Kumar, J. Appl. Phys. **81**, 5821 (1997), and references therein.
[2] Y. Zhang, N. Baruch, and W.I. Wang, Appl. Phys. Lett. **63**, 1068 (1993).
[3] H. Xie and W.I. Wang, Appl. Phys. Lett. **63**, 776 (1993).
[4] U. Cebulla, G. Tränkle, U. Ziem, A. Forchel, G. Griffiths, H. Kroemer, and S. Subbanna, Phys. Rev. B **37**, 6278 (1988).
[5] F.W.O. Da Silva, C. Raisin, S. Gaillard, C. Alibert, and A. Rocher, Thin Solid Films **190**, 21 (1990).
[6] M. Leroux and J. Massies, Appl. Phys. Lett. **68**, 54 (1996); J. Massies, M. Leroux, Y. Martinez, P. Vennegues, and S. Laugt, J. Cryst. Growth **160**, 211 (1996).

[7] O. Madelung, *Semiconductors: Group-IV Elements and III-V Compounds* (Springer, Berlin, 1991), p. 114.
[8] J. Glembocki and B. Shanabrook, in *Semiconductors and Semimetals*, edited by D. G. Seiler and C. L. Littler (Academic, Boston, 1992), Vol. 36, p. 221.
[9] J.S. Hwuang, S.L. Tyan, M.J. Lin, and Y.K. Su, Solid State Commun. **80**, 891 (1991).
[10] S. Iyer, S. Mulugeta, J. Li, B. Mangalam, S. Venkatraman, and K. K. Bajaj, in *Infrared Applications of Semiconductors II,* edited by D. L. McDaniel, Jr., M. O. Manasreh, R. H. Miles, and S. Sivananthan, MRS Symposia Proceedings No. 484 (Materials Research Society, Pittsburgh, 1998), p. 57.
[11] M. Geddo, R. Ferrini, M. Patrini, S. Franchi, A. Baraldi, and R. Magnanini, Appl. Phys. Lett. **73**, 1254 (1998).
[12] A. Bosacchi, S. Franchi, P. Allegri, V. Avanzini, A. Baraldi, C. Ghezzi, R. Magnanini, A. Parisini, and L. Tarricone, J. Cryst. Growth **150**, 844 (1995).
[13] R. Ferrini, G. Guizzetti, M. Patrini, A. Bosacchi, S. Franchi, and R. Magnanini, Solid State Commun. **101**, 93 (1997).
[14] V. Bellani, S. Di Lernia, M. Geddo, G. Guizzetti, A. Bosacchi, S. Franchi, and R. Magnanini, Solid State Commun. **104**, 81 (1997).
[15] J.L. Shay, Phys. Rev. B **2**, 803 (1970).
[16] C. Bocchi, S. Franchi, F. Germini, A. Baraldi, R. Magnanini, D. De Salvador, M. Berti, and A. V. Drigo (unpublished).
[17] Y.S. Tang, J. Appl. Phys. **69**, 8298 (1991).
[18] F. H. Pollak, in *Handbook on Semiconductors*, edited by P. Balkansky (North-Holland, Amsterdam, 1994), Vol. 2, p. 527.
[19] V. Bellani, M. Geddo, G. Guizzetti, S. Franchi, and R. Magnanini Phys. Rev. B **59**, 12 272 (1999).
[20] D.E. Aspnes, Surf. Sci. **37**, 418 (1973).
[21] D.E. Aspnes, Phys. Rev. B **10**, 4228 (1974).
[22] B.V. Shanabrook, O.J. Glembocki, and W.T. Beard, Phys. Rev. B **35**, 2540 (1987).
[23] H. Shen, S.H. Pan, F.H. Pollak, and R.N. Sacks, Phys. Rev. B **37**, 10 919 (1988).
[24] F.H. Pollak, Mater. Sci. Eng., R. **10**, 275 (1993).
[25] C. Bocchi, A. Bosacchi, S. Franchi, S. Gennari, R. Magnanini, and A.V. Drigo, Appl. Phys. Lett. **71**, 1549 (1997).
[26] C. Ghezzi, R. Magnanini, A. Parisini, B. Rotelli, L. Tarricone, A. Bosacchi, and S. Franchi, Phys. Rev. B **52**, 1463 (1995).
[27] Y.S. Huang, H. Qiang, F.H. Pollak, G.D. Pettit, P.D. Kirchner, J.M. Woodall, H. Stragier, and L.B. Sorensen, J. Appl. Phys. **70**, 7537 (1991).
[28] P.W. Chye, I. Lindau, P. Pianetta, C.M. Garner, C.Y. Su, and W.E. Spicer, Phys. Rev. B **18**, 5545 (1978).
[29] G. Bastard, *Wave Mechanics Applied to Semiconductor Heterostructures* (Les Editions de Physique, Paris, 1992).
[30] J. Singh and K.K. Bajaj, J. Appl. Phys. **57**, 5438 (1985); Appl. Phys. Lett. **44**, 805 (1984).
[31] M. Cardona, *Modulation Spectroscopy* (Academic Press, New York, 1969), pp. 122 and 169.
[32] C. Alibert, A. Joulliè, A.M. Joulliè, and C. Ance, Phys. Rev. B **27**, 4946 (1983).
[33] H. Xie, J. Katz, W.I. Wang, and Y.C. Chang, J. Appl. Phys. **71**, 2844 (1992).
[34] P.V. Giugno, A.L. Convertino, R. Rinaldi, R. Cingolani, J. Massies, and M. Leroux, Phys. Rev. B **52**, R11 591 (1995).
[35] R.L. Green, K.K. Bajaj, and D.E. Phelps, Phys. Rev. B **29**, 1807 (1983).